Real-Time Energy Management of a Stand-Alone Hybrid Wind-Microturbine Energy System Using Particle Swarm Optimization

S.A. Pourmousavi, *Student Member, IEEE*, M.H. Nehrir, *Fellow*, *IEEE*, C.M. Colson, *Student Member, IEEE*, and *C.* Wang, *Senior Member*, *IEEE*

***Abstract*—Energy sustainability of hybrid energy systems is essentially a multi-objective, multi-constraint problem, where the energy system requires the capability to make rapid and robust decisions regarding the dispatch of electrical power produced by generation assets. This process of control for energy system components is known as energy management. In this paper, the application of particle swarm optimization (PSO), which is a biologically-inspired direct search method, to find real-time optimal energy management solutions for a stand-alone hybrid wind–microturbine energy system is presented. Results demonstrate that the proposed PSO-based energy management algorithm can solve an extensive solution space while incorporating many objectives such as: minimizing the cost of generated electricity, maximizing microturbine operational efficiency, and reducing environmental emissions. Actual wind and end-use load data were used for simulation studies and the well-established sequential quadratic programming (SQP) optimization technique was used to validate the results obtained from PSO. Promising simulation results indicate the suitability of PSO for real-time energy management of hybrid energy systems.**

***Index Terms*—battery bank, microturbine, optimization methods, real-time energy management, wind power generation.**

I. INTRODUCTION

Increasingly, forces such as cost, environmental concerns, and technological availability are exerting influence on power system design and implementation. Localized frameworks that combine diverse generation and storage components in a microgrid architecture, known as energy systems, are emerging to offer electrical consumers the opportunity to tailor their installed assets to meet local requirements. Renewable energy power generation sources such as wind and solar photovoltaic (PV), and emerging low- or zero-emission power generation devices, such as microturbine (MT) and fuel cells (FC), fall in this category. These energy sources can complement each other to overcome the variable nature of the renewable energy sources, and together with energy storage (ES), improve system reliability and energy sustainability to the maximum extent possible. Such systems can be used stand-alone as independent microgrids for electrifying remote areas far from the grid, e.g. [1]-[4], or to serve a collection of loads in the urban areas, in grid–connected or island mode, e.g. [5], [6]. In either case, proper unit sizing of the available energy sources is necessary to ensure that proper generation capacity is available for a particular application. Extensive work has been done in this area, e.g. [7]-[12]; many dependable computer-based programs are also available for this purpose, e.g. [13]-[15].

Effective energy management of hybrid energy systems is necessary to ensure optimal energy utilization and energy sustainability to the maximum extent. Furthermore, given the intermittent nature of the renewable energy resources involved and the multiple objectives that need to be satisfied (some of which may be conflicting), the energy management system (EMS) is complex and needs to find solutions quickly and continuously, e.g. every minute or few minutes. In general, conventional optimization techniques are too slow to be used for real-time optimization of the subject multi-objective, multi-constraint energy management problem. As a result, recently, research in this area has been focused on the application of intelligent control for unit sizing and energy utilization of hybrid energy systems, e.g. [16]-[20]. However, most of the reported work is on off-line applications such as generation unit sizing and optimal power dispatch, and little work has been reported on real-time management of energy systems using multi-objective optimization [5], [21].

This paper targets the real-time application of a heuristic multi-objective optimization technique, particle swarm optimization (PSO) [22], [23], for energy management of a hybrid energy system, which is achieved in a small fraction of a second. A hybrid stand-alone wind-MT-ES system is considered to supply the equivalent load requirements of a 120-home residential neighborhood, shown in Fig. 1. The primary components of the system are a wind energy conversion system (WECS) that utilizes a self-excited

This work was supported by Pacific Northwest National Laboratory, which is operated for the U.S. Department of Energy by Battelle under Contract DE-AC05-76RL01830.

S.A. Pourmousavi (e-mail: s.pourmousavikani@msu.montana.edu), M.H. Nehrir (e-mail: hnehrir@ece.montana.edu), and C.M. Colson (e-mail: christopher.colson@msu.montana.edu) are with the Electrical and Computer Engineering Department, Montana State University, Bozeman, MT 59717 USA.

C. Wang is with the Division of Engineering Technology and the Department of Electrical and Computer Engineering, Wayne State University, Detroit, MI 48202 USA (e-mail: cwang@wayne.edu).

induction generator (SEIG) [1],[4], a single-shaft microturbine generator (MTG) that incorporates a SEIG as well [1], and a battery bank. The ratings of these components used in this study are given in the Fig. 1. However, the proposed intelligent energy management system (EMS) described in the paper can be applied to other WECS and MT configurations, such as a WECS or a MT which utilize a permanent magnet synchronous generator, and to other hybrid systems.

The study reported in this paper is the continuation of a previous work by the authors [1], where the design of an EMS for a hybrid wind-MT energy system is reported; however, no optimization was used in that reference. In the current paper, a real-time PSO-based EMS for the hybrid wind-MT-ES system is proposed. In addition, the well-established analytical optimization technique, sequential quadratic programming (SQP) [25], was also used to validate the results obtained using PSO. Actual wind and end-use load data were used in the simulation studies, conducted in the MATLAB/Simulink® environment.

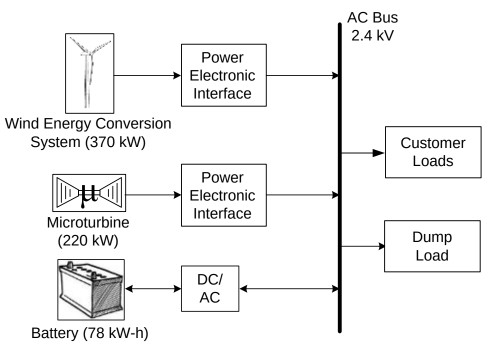

Fig. 1. Configuration of the proposed system.

The objective function for both optimization algorithms (PSO and SQP) used is updated every three minutes, during which load and generation are considered constant. The choice to update the optimization at a smaller interval is possible, but at the expense of longer simulation time. The storage battery bank was used to ensure long-term energy sustainability and to supply the power needed during each interval to cover short-duration transients caused by sudden changes in load or wind speed. The extremely fast convergence speed of PSO [33] and the promising simulation results obtained show the potential of this multi-objective optimization technique for real-time energy management of multi-source energy systems. It should be noted that the focus of the reported work is on energy management, where 24-hour simulation studies were conducted. Unit sizing and system voltage and frequency characteristics and stabilization are not discussed in this paper and will be reported in a future work.

This paper is organized as follows. Formulation of the optimization problem is discussed in Section II. Section III gives a description of the proposed EMS. In Section IV, PSO is briefly discussed and, PSO-based energy management is presented. Simulation results are given in Section V. A discussion is presented in Section VI and concluding remarks are given in Section VII.

II. Formulation of the Optimization Problem

The objective function developed for the EMS for the hybrid system presented here takes into account a number of factors including: the cost of energy produced by the WECS and MT, as well as the technical constraints of the optimization procedure. In this section, the cost functions for the MT and WECS and the required constraints are developed.

a. MT Cost Function and Constraints

The MT cost function can be expressed as follows [5]:

$$F_{t,MT} = C_{MT} . F_{MT} . P_{t,MT} . \Delta T + OM_{t,MT} + SC_{t,MT} \qquad (1)$$

where,

- $F_{t,MT}$ is the total operating cost of the MT ($).
- C_{MT} is the fuel cost of the MT unit ($/m^3). Natural gas was used as fuel at a cost of 0.3571 $/m^3 [26].
- F_{MT} is the fuel consumption rate (m^3/kWh). $F_{MT} = 0.85$ m^3/kWh was used in this study [21].
- $P_{t,MT}$ is a decision variable representing the real power output from the MT unit (kW).
- ΔT is the energy management time step which is set at 3 minutes in this study (h), i.e. the optimization is updated every 3 minutes.
- $OM_{t,MT}$ is the operation and maintenance (O & M) cost of the MT unit ($).
- $SC_{t,MT}$ is the start up cost of the MT unit ($).

The O & M cost of the MT is assumed to be proportional with the produced energy [5], [27]:

$$OM_{t,MT} = K_{OC} . P_{t,MT} . \Delta T = 0.00587 \times P_{t,MT} . \Delta T \qquad (2)$$

where, the proportionality constant, K_{OC} is taken as 0.00587 $/kWh for MT [5]. The start-up cost of the MT depends on the length of time the unit has been turned off before start-up once again [5], [28]:

$$SC_{t,MT} = \left(\sigma_{MT} + \delta_{MT} \left(1 - e^{-\tau_{off,MT} / \tau_{MT}} \right) \right) . \left(1 - u_{(t-1),MT} \right) \qquad (3)$$

where, σ_{MT} and δ_{MT} are the hot start-up and cold start-up costs for the MT, respectively. τ_{MT} is the MT cooling time constant, $\tau_{off,MT}$ is the time the MT has been off, and $u_{(t-1),MT}$ shows the status of the MT (being on or off) at time step *t-1*. If cold start-up of the MT requires power to run the MT's auxiliary systems [29], then the WECS or battery is required to provide this cold start-up power. In this study, the MT's hot start-up time is 30 sec, cold start-up time is 200 sec, and its cooling time constant is 520 sec [29]. In general, for optimization studies that include MT, hot and cold start-up costs should be included, however in this particular case the value of these parameters do not affect the optimization results, because the fuel cost of the MT {i.e., the first term on the right side of (1)} is always higher than the total cost of operating the WECS.

Emissions cost has not been considered in this work because of unavailability of data or function [29]; however, if such data or function is available, an expression for this cost can be added to the objective function (1) .

The output power of the MT unit in stable operation is restricted by its lower and upper limits as follows:

$$P_{MT}^{\min} \le P_{t,MT} \le P_{MT}^{\max} \tag{4}$$

In our case, the maximum available power from the MT is 220 kW and the lower limit is zero, i.e. the MT can be turned off when the output power from the WECS is enough to meet the demanded power. Once the MT is switched on ($u_{t,MT}$=1), it has to operate continuously for a certain length of time before being switched off ($u_{t,MT}$=0). Also, a certain off-time period has to be achieved, meaning that the MT must be off for a certain period before being restarted. Violation of such constraints can shorten the unit's life time. These constraints are formulated as continuous run/stop time constraints as follows:

- Evaluate whether the MT may be shut off by comparing the on-time of the MT in the previous steps of the energy management with the MT's minimum up-time (MUT_{MT}):

$$if\ \left(T_{MT}^{on} - MUT_{MT}\right) \ge 0, Then\ T_{MT}^{on} = 0,\ u_{t,MT} = 0 \tag{5}$$

- Evaluate whether the MT may be started up by comparing the off-time of the MT in the previous time steps with the MT's minimum down-time (MDT_{MT}):

$$if\ \left(T_{MT}^{off} - MDT_{MT}\right) \ge 0, Then\ T_{MT}^{off} = 0, u_{t,MT} = 1 \tag{6}$$

where T_{MT}^{on} , T_{MT}^{off} (sec.) are the time length the MT has been on or off, respectively. In this study MUT_{MT} = 600 sec. and MDT_{MT} = 300 sec. [29]. Also, the number of starts and stops should not exceed a certain maximum depending on the MT specifications [5]:

$$\varepsilon_{start-stop} \le N_{\max} \tag{7}$$

where $\varepsilon_{start\text{-}stop}$, is the number of start-stops during simulation, and N_{max} is the maximum number of start-stops. In this study, N_{max} =30, which is never reached.

b. WECS Cost Function and Constraints

The following cost function is used for the WECS [20]:

$$F_{t,WT} = C_{WT} .P_{t,WT} .\Delta T \tag{8}$$

where $F_{t,WT}$ is the cost of wind-generated energy, $P_{t,WT}$ and C_{WT} are the WECS' wind power (kW) and its cost coefficient for the generated energy at each time step ($/kWh), respectively. In this study $F_{t,WT}$ is always less than $F_{t,MT}$. The value of C_{WT} depends on the actual cost of the wind-generated energy, which, in this case, is taken as $0.1/kWh. Again, this factor will not affect the results since $F_{t,WT} < F_{t,MT}$.

The output power of the WECS is restricted based on its power curve and parameters. The following parameters are used in this study [1]:

- Cut-in speed, $v_{cut\text{-}in}$ =3 m/s,
- Rated speed, v_{rated} =14 m/s,
- Cut-out speed, $v_{cut\text{-}out}$ =25 m/s.

The WECS does not generate any power for $v_{wind} < v_{cut\text{-}in}$. Pitch control is used to limit the output power of the WECS to its rated value (370 kW) when $v_{rated} < v_{wind} < v_{cut\text{-}out}$, and the WECS output power is zero for $v_{wind} > v_{cut\text{-}out}$. The details of the WECS modeling are given in [30]. The WECS output power is calculated at each time step using the wind speed at that instant. The power balance (equality constraint) for the WECS and MT to meet the load demand is:

$$P_{t,MT} + P_{t,WT} = P_{t,Load} \tag{9}$$

$$0 \le P_{t,WT} \le P_{t,WT}^{\max} \tag{10}$$

where, $P_{t,Load}$ is the load demand at each time step. Proper optimization techniques can then be used to best share power amongst the generation sources of the hybrid system to minimize the cost of electricity while satisfying the equality and inequality constraints given above. According to the following objective function, total operational cost is minimized:

$$Min.\ Objective\, Func. = F_{t,MT} + F_{t,WT} \tag{11}$$

III. THE PROPOSED REAL-TIME EMS

The flowchart for the proposed energy management, which accounts for multiple simultaneous objectives for the hybrid energy system, is annotated in Fig. 2. As shown in this figure, the battery has three states; charging, discharging and inactive. The battery is in the inactive or charging mode in *scenarios* 1 and 2, and in discharging mode in *scenario* 3. The primary objectives of the EMS are as follows:

- Minimize the cost of energy generation,
- Maximize battery life by monitoring and controlling its state of charge (SOC) and charge/discharge process,
- Maximize the use of excess available wind power in a useful dump load when the battery is fully charged in an attempt to increase system utilization [34],
- When the MT is in operation, adjust its operating point to near its rated power to increase its operation efficiency and reduce its environmental impact, [29],
- Maximize the average available stored energy in the battery (i.e., higher battery SOC), hence improving system reliability.

At the start of the proposed energy management algorithm, the boundary equations for the energy sources involved and the equality constraints are defined as follows:

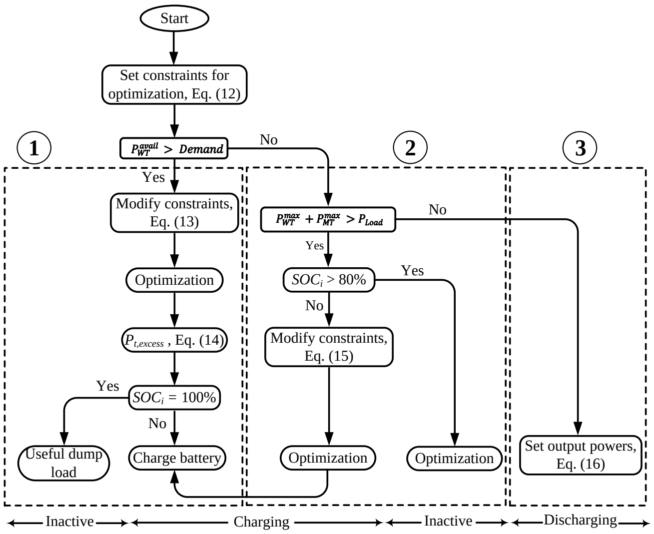

Fig. 2. Proposed energy management strategies for the WECS-MT-ES-EWH system.

$$\begin{cases} P_{t,WT}^{max} = P_{t,WT}^{avail}\ ,\ \ P_{WT}^{min} = 0; \\ P_{MT}^{rated} = 220\ kW\ ,\ \ P_{t,MT}^{min} = 0, \\ P_{t,supply} = Demand_t\ ,\ \ P_{t,supply} = P_{t,WT}^{optim} + P_{t,MT}^{optim} \pm P_{t,batt} \end{cases} \tag{12}$$

- where $P_{t,WT}^{max}$ and $P_{t,WT}^{min}$ are the maximum and minimum wind power limitations for the WECS, respectively;
- P_{MT}^{rated} and $P_{t,MT}^{min}$ are the maximum (rated) and minimum power limitation for the MT;
- $P_{t,supply}$ is the overall power demand of the hybrid system, including power supplied to the load, dump load, and to the battery;
- $Demand_t$ is the power demanded by the load at time *t;*
- $P_{t,WT}^{optim}$ and $P_{t,MT}^{optim}$ are the optimized share of the WECS and the MT after optimization;
- $P_{t,batt}$ is the amount of charge/discharge power to/from the battery.

Scenario 1: As shown in Fig. 2, if the maximum available power from the WECS is greater than demand, there is excess power available from the WECS which can be used to charge the battery, if needed. Otherwise, the excess power is supplied to a useful dump load, e.g. an auxiliary electric water heater (EWH) to preheat water, as proposed in [34]. Therefore, the actual demand is set to the available power from the WECS, i.e. the equality constraint (eq. 9) of the optimization will change to:

$$P_{t,supply} = P_{t,WT}^{avail} \tag{13}$$

After performing optimization, the excess available power is the difference between the total generation and demand as follows:

$$P_{t,excess} = P_{t,WT}^{optim} + P_{t,MT}^{optim} - Demand_t \tag{14}$$

As shown in Fig. 2, the excess power is used to charge the battery, if the battery is not fully charged. Otherwise, the battery will remain inactive and the excess power is directed to the useful dump load. In this operation mode, the mechanical stress on the wind turbine is reduced because the WECS output power is not limited by pitch control.

Scenario 2: In cases where power from the WECS is not enough to meet the demand, the MT will be turned on. In this case, if the total power from the WECS and MT is greater than demand and the battery SOC is higher than 80%, the battery remains inactive and the optimization procedure will be performed to determine the generation dispatch of the WECS and MT. If the battery SOC is lower than 80%, the optimization constraints will be changed as follows:

$$\begin{cases} P_{t,batt}^{min} = 1\ kW \\ P_{t,supply} = P_{t,WT}^{max} + P_{t,MT}^{rated} \end{cases} \tag{15}$$

This way, the excess power will be used to charge the battery bank, which can increase the reliability of the whole system, resulting in improved energy sustainability. According to [35], recharging lead-acid batteries immediately after discharging will extend battery life significantly. In order to avoid charging the battery at very low currents, which can reduce the battery lifespan, the lower limit of the battery charging power is arbitrarily set to 1 kW (about 3 A). Also, the upper battery charge power is limited to 62.4 kW (about 200 A) to keep the battery in safe condition. Note that this strategy is only applied when the MT is already turned on to meet a part of the demand, because turning on the MT only for charging the battery will add hot start-up cost to the energy production cost. Moreover, the number of starts and stops of the MTG can affect its life and efficiency. Cost analysis of MT operation is beyond the scope of this paper and has not been carried out.

Scenario 3: If the total power from the WECS and MTG is less than demand, the battery needs to be discharged to meet demand. In this condition, optimization is not necessary and the output power from the WT, MT, and battery is as follows:

$$\begin{cases} P_{WT}^{optim} = P_{WT}^{avail} \\ P_{MT}^{optim} = P_{MT}^{rated} = 220\ kW \\ P_{batt} = Demand - P_{WT}^{optim} - P_{MT}^{optim} \end{cases} \tag{16}$$

In this study, two optimization techniques are used: the evolutionary algorithm, PSO, and the conventional technique, SQP. PSO is the main optimization algorithm used; it is described in Section IV. The PSO-based EMS developed for this study, is described in Subsection IV-a. SQP-based EMS is used to verify the results of the PSO-based strategy.

IV. Particle Swarm Optimization

The PSO algorithm is performed at each time step (every 3 minutes) to determine the optimum balance of WECS and MT to meet demand. Wind speed data, demand data, status of the MT, and the battery SOC are the input values to the optimization block. The battery model used and the method of calculating battery SOC are available in MATLAB/Simulink SimPowerSystems toolbox [31]. Since the proposed optimization system operates in real-time, fast and accurate optimization methods should be employed. If any changes in demand or wind speed occur during the optimization intervals, the storage battery will respond to the power transients.

PSO is a population based stochastic optimization technique developed by Kennedy and Eberhart [32], inspired by social behavior of bird flocking, fish schooling and swarm theory. PSO shares many similarities with evolutionary computation techniques such as genetic algorithms (GA). The system is initialized with a population of random solutions and searches for optima by updating generations. However, unlike GA, PSO has no evolution operators such as crossover and mutation. In PSO, the potential solutions, named as particles, 'fly' through the problem space following the current optimum particles. Each particle is regarded as a point in a d-dimensional space that adjusts 'flying' according to its own flying experience and flying experience of other particles.

PSO is simple in concept. It has few parameters to adjust and is easy to implement. In the past several years, PSO has been successfully applied in many research and application areas. In general, all the application areas that the other evolutionary application techniques are good at are the application areas for PSO. Reference [33] gives a comprehensive overview of PSO and its applications in power systems, and discusses its fast convergence speed and advantage over stochastic methods.

The original PSO maintains a population of particles (x_1, x_2, ⋯, x_p) which are initially distributed uniformly around the search space. Each particle represents a potential solution to the optimization problem. Let p be the size of the swarm. For each particle i, the position x_i is updated as follows [22], [32]:

$$x_{k+1}^{i} = x_{k}^{i} + v_{k+1}^{i} \tag{17}$$

Each particle in PSO is associated with a pseudo-velocity $v_{k+1}^{i}\left(-v_{max}^{i} \le v_{k+1}^{i} \le v_{max}^{i}\right)$, which represents the rate of the position change for the particle [22], [32]:

$$v_{k+1}^{i} = \omega_k v_k^i + c_1 r_{1,k}\left(p_k^i - x_k^i\right) + c_2 r_{2,k}\left(p_k^{gi} - x_k^i\right) \tag{18}$$

Equation (18) is used to calculate each particle's new velocity v_{k+1}^{i} based on its previous velocity v_k^i and the distances of its current position x_k^i from its own best experience (position) and the best experienced position of its own informants, p_k^{gi}, according to Fig. 2(a). Here, subscript k and i indicate a pseudo-time increment and the number of particles, respectively; r_1 and r_2 represent uniform random numbers between 0 and 1, which will be regenerated at each iteration. c_1 and c_2 are two positive constants, called the cognitive and social parameter, respectively (in this study, they are chosen as c_1=1.5 and c_2=1.5) [22], [32].

Initially (at time step t=0), the particles' velocities, v_0^i, are random numbers within the boundary $0 \le v_0^i \le v_{max}^i$. The maximum velocity v^{max} allowed actually serves as a constraint that controls the maximum global exploration ability PSO can have. Then, each particle flies toward a new position according to (17) and (18). The inertia weight ω_k in (18) should be neither too large, which could result in premature convergence, nor too small, which can slow down convergence excessively (they are chosen as ω_{min}=0.6 and ω_{max}=1.2; ω holds the ω_{min} value at the beginning of each simulation cycle and increases linearly to ω_{max} at the end) [22]. Therefore, the particles have a tendency to fly towards better and better search areas over the course of the search process. As a result, the search can always reach an optimum or a solution very close to the optimum using fewer fitness evaluations [22].

The performance of each particle is measured according to a predefined fitness function, which is related to the problem to be solved. Each particle moves around the search space updating its velocity and position based on the best positions (P_{best}) thus far discovered by itself and by its informants. If all the particles are informed by each other, all the information acquired is disseminated immediately. This is a favorable scenario; however, it is highly risky to have a behavior that is too uniform, i.e. when all the particles will act uniformly [22]. Conversely, if each particle has too few informants, more diversified behaviors will be obtained. This scenario carries the risk that poor information can be transmitted.

In this study, the information links between the particles were defined once (and kept unchanged throughout the simulation), generally according to the "circular" diagram shown in Fig. 2(b) [22].

The N particles of the swarm are laid out virtually on a circle, and numbered sequentially from 1 by traversing the circle. Each particle has a set of informants of fixed size K.

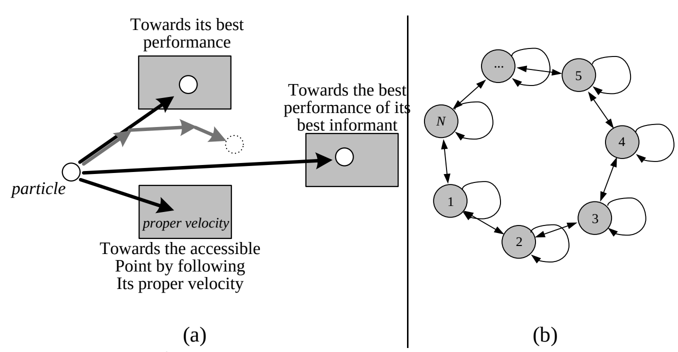

Fig. 3. (a) Three fundamental elements the particles position updating, (b) graph of influence of a swarm of N particles in circular form with three informants for each particle [22].

The neighborhood of size K of a particle is obtained from the virtual circle by recruiting alternately on the right and left of its position, until a total of $K-1$ neighbors are obtained. The particle itself is also included, i.e. K=3. In this study, a swarm with 5 particles is used. Handling PSO by informant configuration, shown in Fig. 2(b), leads us to differentiate properly between the two functions provided by the particles: exploring the search space and memorizing the best position, P_{best}, found during this search. These two functions are carried by distinct particles [22].

a. PSO-based Energy Management

To apply PSO to the WECS-MT energy management problem at hand, $P_{t,WT}$ is selected as a decision variable to be optimized by PSO. The variable, $P_{t,MT}$ is then computed using the equality constraint given by (9). To optimize the problem in each step, initial swarms are defined as follows:

$$P_{t,WT} = rand() \times \left(P_{t,WT}^{avail} - P_{WT}^{min}\right) + P_{WT}^{min} \tag{19}$$

where *rand()* represents uniform random numbers between 0 and 1, $P_{t,WT}^{avail}$ is the maximum available power from the WECS, which is calculated by the algorithm given in Fig. 2 using wind speed data. Then, the output power of the MT can be calculated as follows:

$$P_{t,MT} = P_{t,Load} - P_{t,WT} \tag{20}$$

Given that the energy resource (wind) for the WECS is free and environmentally friendly, the overall objective of the WECS-MT system is to operate the WECS to the full capacity needed and operate the MT when the WECS cannot supply all the demanded power by itself. Two energy management scenarios are considered:

Case 1, no optimization, WECS-MT-ES. In this case, the WECS power will supply the load and if excess power is available, it will be used to charge the storage battery if it is not fully charged (SOC=100%). Otherwise, the WECS output power is limited to that required by the load. The MT will be used when the combination of WECS and battery power is not sufficient to supply the load. Therefore, the WECS maximum power dispatch is governed by the following equation:

$$\begin{cases} If \;\; P_{t,WT}^{avail} > P_{t,Load} \;\;\&\;\; SOC_t = 100\% \Rightarrow P_{t,WT}^{max} = P_{t,Load} \\ \qquad\qquad else: \quad P_{t,WT}^{max} = P_{t,WT}^{avail} \end{cases} \tag{21}$$

This case is similar to that presented in [1]. Its disadvantage is that when the available wind power is greater than demand and the battery is fully charged (i.e. when (21) is not satisfied), then the WECS power must be limited.

Case 2, optimized, WECS-MT-ES-dump load: This is the preferred energy management strategy, where the maximum available power is extracted from the WECS at all times. If the available wind power is more than load demand and the storage battery is full, the excess available power of the WECS is supplied to a useful dump load. In a previous study by the second author, it has been shown that an auxiliary EWH can be used as a useful dump load [34]. Any excess available wind power will be supplied to the auxiliary EWH to pre-heat the water before entering the main residential EWH. It has been shown in [34] that the energy used by the main residential EWH can be reduced considerably by using an auxiliary EWH as a dump load. This scenario is adapted in the *Case 2* study.

In the PSO algorithm, the values of initial guesses used for the objective functions are assigned by intuition (best guess). The best possible answer will then be selected and the swarms' positions will be updated, for each decision variable according to (17) and (18). The following equality constraints are applied at each iteration to modify the swarms' positions:

$$if \quad P_{t,MT} < 0 \rightarrow \begin{cases} P_{t,WT} = P_{t,WT} - \left|P_{t,MT}\right| \\ P_{t,MT} = 0 \end{cases} \tag{22}$$

$$if \quad P_{t,WT} > P_{t,WT}^{max} \rightarrow \begin{cases} P_{t,MT} = P_{t,MT} + \left(P_{t,WT}^{max} - P_{t,WT}\right) \\ P_{t,WT} = P_{t,WT}^{max} \end{cases} \tag{23}$$

The above equality constraints ensure that improper selections for $P_{t,MT}$ and $P_{t,WT}$ values are adjusted into the space of appropriate dispatch assignments. The flowchart for the proposed PSO algorithm is illustrated in Fig. **4**. For the initial searching points, 5 swarms and 50 iterations are used. These values are chosen by experience; caution must be taken to ensure that the solution converges within the maximum number of iterations. In this study, when the above values were used, the optimal solution was reached within 0.012 sec.

As stated earlier, the well-established analytical optimization algorithm, SQP, which is available in MATLAB, is used to validate the results obtained using PSO. SQP is applied to show the accuracy and fast convergence time of PSO. SQP optimization is based on quadratic programming which uses a Quasi-Newton method. Detailed description of SQP is beyond the scope of this paper; interested readers are referred to the comprehensive literature available on this optimization technique, e.g. [25].

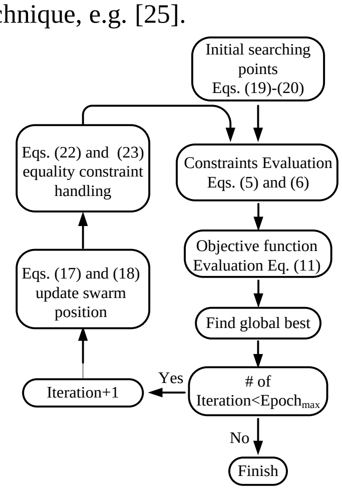

Fig. 4. Flow chart for the proposed PSO algorithm.

V. Simulation Results

The stand-alone wind-MT-ES system in this study is designed to supply power to a residential neighborhood in the

U. S. Pacific Northwest area consisting of 120 houses. The typical average residential daily load demand profile used is obtained from the Pacific Northwest regional information reported in [36]. The total aggregate hourly average load demand of the residential neighborhood is shown in Fig. 5.

Actual wind data is used in this case study, obtained from the online records of the weather station at Deer Lodge, Montana, affiliated with the Pacific Northwest Cooperative Agricultural Weather Network (AgriMet) [37]. The hourly average wind speed data, recorded on March 12, 2007 at a height of 2 meters, was chosen for the 24-hour simulation study. This date was chosen because its 24-hour average wind speed closely matched the annual average wind speed for the area. The wind data on this date was also used in the study (by the authors) reported in [1], which would make the comparison of the results obtained using the proposed EMS with those reported in [1] easier. Data reported in [37] was corrected for the proposed wind turbine hub height of 40 meters, shown in Fig. 6, using the following expression [38]:

$$v_{s1} = v_{s0} \cdot \left(\frac{H_1}{H_0} \right)^{\alpha} \tag{24}$$

where v_{s1}, v_{s0} (m/sec) are wind speeds at the hub height H_1 and the height H_0 (m) at which the data was collected. α is the wind speed correction exponent; in this study, α sets to 0.13 [7], [38].

The energy management algorithm discussed in the previous section is used with PSO and SQP optimization techniques, and simulation results were compared with those reported in [1], where no optimization was used (i.e., *case 1*- no optimization- in this study).

Fig. 7 shows the output power of the WECS corresponding to the wind speed profile shown in Fig. 6. It is noted that the wind power profiles for the proposed EMS (PSO- and SQP-based EMS) are exactly the same (PSO-based is shown as a grey line; SQP-based is highlighted with circles), but the power profile is slightly different under no optimization (i.e., during the periods 9:30-10:30, 12:30-15:00 and 16:00-16:30), where the responses are shown with solid (dark) line. In the first high-wind period (9:30-10:30 hr), the excess power from the WECS is higher than the battery charging limit. Therefore, the WECS power is limited (by pitch control) to the amount of demand plus maximum battery charging power. Similarly, in the next high-wind period (12:30-15:00 hr and 16:00-16:30 hr), the WECS output power is more than demand and the battery is fully charged. Therefore, in the no optimization scenario, the output power from the WECS is further limited by pitch controller as described in [30], whereas, in the case of the proposed EMS, the excess wind power available in the same periods is delivered to the useful dump load, as shown later in Fig. 11. During the periods 10:00-10:30 and 12:30-15:00, the available wind power is higher than the WECS rated power. Therefore, pitch control is applied to limit the WECS power to its rated value.

Fig. 8 shows the MTG output power profile for the three scenarios explored. In most cases, the MTG produces power when the available wind power is not sufficient to meet the demand. However, under the proposed EMS (using PSO or SQP), when the MT is operating and the battery SOC is below 80%, the MT will operate at rated power to take advantage of improved efficiency and reduced emission [29], and the excess available power is used to charge the battery (Fig. 8, 2:30-3:30, 19:30-21:00, and 23:30-24:00 hr).

Fig. 9 shows the SOC of the battery for the three scenarios studied. The initial battery SOC is assumed to be 50% to better show its charge/discharge pattern. From the results shown, the superiority of the optimized energy management scenarios (in keeping the battery SOC higher) over when no optimization is used is clear. Because of its improved SOC profile, the battery is in a better state of health, and has a longer lifespan [35].

Fig. 10 shows the battery power profile for the three scenarios. In the no optimization scenario, the battery will charge when the WECS power is in excess of demand (0:00-2:00, 9:00-11:00, 12:00-12:30 hr) and will discharge when the WECS plus MTG cannot meet the power demand (17:00-19:30, 22:00-23:30 hr). In the remainder of the hours, the battery remains idle. Under the proposed EMS, in addition to the above charging periods, the battery is also charged when the WECS plus MTG power is in excess of demand (i.e. 2:00-3:00, 19:30-21:00, and 23:30-24:00 hr). During these periods, the battery is further charged by the MTG since the MTG is operating near its rated power to further charge the battery when the battery SOC is below 80%. As shown in Fig. 10, the battery charging power is limited to 62.4 kW (about 200 A) for safety reasons.

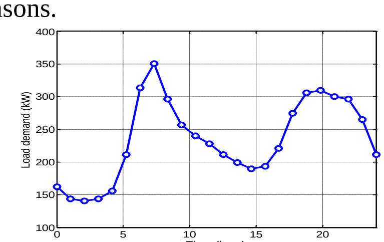

Fig. 5. Hourly average demand of 120 typical residences in the Pacific Northwest area [36].

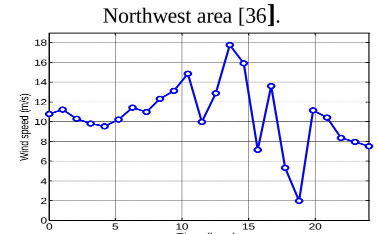

Fig. 6. Actual corrected wind speed data for Deer Lodge, MT on March 12, 2007 [37], corrected to hub height of 40 m.

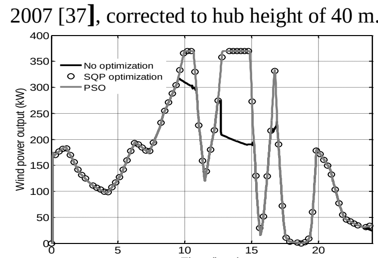

Fig. 7. Wind power output for different management algorithms and optimization methods.

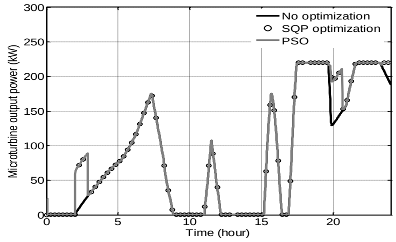

Fig. 8. MTG output power for different management algorithms and optimization methods.

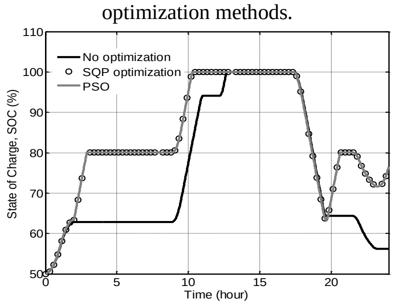

Fig. 9. SOC of battery for different algorithms and optimization methods.

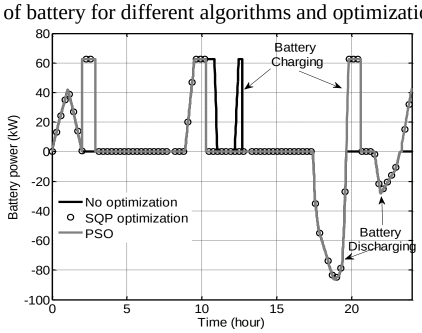

Fig. 10. Battery power for different power management algorithms in a day.

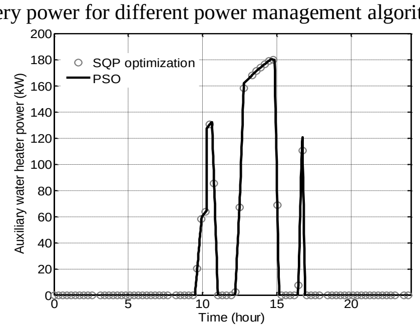

Fig. 11. Auxiliary water heater power for a day in the proposed energy management strategy.

Fig. 11 shows the periods when excess power is available from the WECS or MT. This excess power is delivered to a useful dump load (e.g., an auxiliary EWH) for the PSO and SQP optimization strategies. No useful dump load was considered under the "no optimization" case, reported in [1].

VI. Discussion

A stand-alone hybrid wind-MT-ES system has been used herein to explore the feasibility of a proposed PSO-based energy management algorithm for real-time applications. In this case, since priority is given to wind power production because of obvious advantages, the objective functions defined for the optimization problem are linear. As a result, the simulation results obtained when using the PSO and SQP algorithms are exactly the same. However, in more complex systems, where the objective functions are non-linear, the random nature of the PSO-based EMS can improve the final results in comparison with the analytical-based optimization techniques [33]. It is our plan to apply the proposed PSO-based EMS to more complex multi-source systems in future work.

Because the objective here is to explore the feasibility of application of PSO for real-time EMS, the convergence time of the PSO algorithm is highly important. Table I shows a comparison of the computation time for the PSO- and SQP-based EMS for the wind-MT-ES system. As noted in the table, PSO convergence time is nearly 90 times faster than the analytical SQP optimization. This fast response of the PSO is critically important in its real-time application for energy management of multi-source renewable energy-based systems.

TABLE I
Computation time for different optimization techniques

Optimization Algorithm	PSO	SQP Optimization
Time (seconds)	0.012	0.957

VII. Conclusions

Real-time PSO-based energy management of a stand-alone hybrid wind-MT-ES system is presented in this paper. The developed EMS promotes energy sustainability in two ways: first, by ensuring an optimal balance between the attached generation sources based on the multiple constraints, and secondly, by incorporating desirable energy objectives into the EMS decision-making process. Specifically, the following factors are also considered:

- The use of a useful dump load (an auxiliary EWH) to increase energy efficiency of the system,
- Keeping the operating point of the MT near its rated value when feasible to increase its operation efficiency and reduce its environmental impact,
- Maximizing the average available stored energy in the battery by striving to keep its SOC at 80% or higher, hence improving overall system reliability and increasing the battery life.

Simulation results show the suitability and potential benefits of the proposed PSO-based energy management strategy for the hybrid system.

In order to verify the validity of the proposed approach, simulation results were also obtained for the same system using the well-established SQP optimization and when no optimization was used. Simulation results compare well and show the benefits of the proposed EMS in increasing the overall system reliability and energy sustainability. In particular, the main advantage of the PSO-based energy management strategy is its extremely fast convergence time, which is critically important for real-time energy management applications.

References

[1] Wang, C.; Nehrir, M.H.; Colson, C.M.; Li, J.;"Power management of a stand-alone hybrid wind-microturbine distributed generation system," *Proceedings*, Power Electronics and Machines in Wind Applications (PEMWA 2009), 24-26 June 2009, pp. 1 – 7.

[2] Wai, R.-J.; Lin, C.-Y.; Duan, R.-Y.; Chang, Y.-R.; "High-Efficiency Power Conversion System for Kilowatt-Level Stand-Alone Generation Unit with Low Input Voltage," *IEEE Transactions on Industrial Electronics*, Vol. 55, Issue 10, Oct. 2008, pp. 3702 – 3714.

[3] Valenciaga, F.; Puleston, P.F.; "Supervisor control for a stand-alone hybrid generation system using wind and photovoltaic energy," *IEEE Transaction on Energy Conversion*, Vol. 20, Issue 2, Sept. 2005.

[4] Wang, C.; Nehrir, M.H.;"Power Management of a Stand-Alone Wind/Photovoltaic/Fuel Cell Energy System," *IEEE Trans. On Energy conversion*, vol. 23, Issue 3, Sep. 2008, pp. 957–967.

[5] Mohamed, F.A.; Koivo, H.N.; "MicroGrid Online Management and Balancing Using Multiobjective Optimization," *Proceeding*s, Power Tech 2007, IEEE Lausanne, Switzerland, 1-5 July 2007, pp. 639 – 644.

[6] Katiraei, F.; Iravani, M.R.;"Power Management Strategies for a Microgrid With Multiple Distributed Generation Units," *IEEE Trans. on Power Systems*, vol. 21, Issue 4, Nov. 2006, pp. 1821–1831.

[7] Kellogg, W.D.; Nehrir, M.H.; Venkataraman, G.; Gerez, V.; "Generation unit sizing and cost analysis for stand-alone wind, photovoltaic and hybrid wind/PV systems," *IEEE Trans. On Energy Conversion*, vol. 13, Issue 1, March 1998, pp.70–75.

[8] Nelson, D.B.; Nehrir, M.H.; Wang, C.; "Unit sizing and cost analysis of stand-alone hybrid wind-PV-fuel cell power generation system," *Renewable Energy*, vol. 31, 2006, pp. 1641–1656.

[9] Koutroulis, E,; Kolokotsa, D.; Potirakis, A.; Kalaitzakis, K.; "Methodology for optimal sizing of stand-alone photovoltaic/wind-generator systems using genetic algorithms," *Solar Energy*, vol. 80, 2006, pp. 1072–88.

[10] Yang, H.; Zhou, W.; Lu, L.; Fang, Z.; "Optimal sizing method for stand-alone hybrid solar–wind system with LPSP technology by using genetic algorithm," *Solar Energy*, vol. 82, 2008, pp. 354–67.

[11] Lingfeng, W.; Singh, C.; "Multicriteria Design of Hybrid Power Generation Systems Based on a Modified Particle Swarm Optimization Algorithm," *IEEE Trans. On Energy Conversion*, Vol. 24, Issue 1, March 2009, pp. 163 – 172.

[12] Kashefi, A.; Riahy, G.H.; Kouhsari, S.M.; "Optimal design of a reliable hydrogen-based stand-alone wind/PV generating system, considering component outages," *Renewable Energy*, vol. 34, Issue 11, Nov. 2009, pp. 2380-2390.

[13] Online, HOMER Energy LLC, http://homerenergy.com/about.asp, software developed by National Renewable Energy Laboratory (NREL).

[14] Online, DER-CAM - Distributed Energy Resources Customer Adoption Model, http://der.lbl.gov/dercam.html, software developed by Lawrence Berkeley National Laboratory (LBNL).

[15] Marnay, C.; Venkataramanan, G.; Stadler, M.; Siddiqui, A.S.; Firestone, R.; Chandran, B.; "Optimal Technology Selection and Operation of Commercial-Building Microgrids," *IEEE Transactions on Power Systems*, vol. 23, Issue. 3, Aug. 2008, pp. 975-982.

[16] Miranda, V.; Pun Sio, H.; "Economic dispatch model with fuzzy wind constraints and attitudes of dispatchers," *IEEE Trans. On Power Systems*, vol. 20, Issue 4, Nov. 2005, pp. 2143 – 2145.

[17] Chen, C.L.; "Simulated annealing-based optimal wind-thermal coordination scheduling, Generation," *Transmission & Distribution, IET*, vol. 1, Issue 3, May 2007, pp. 447 – 455.

[18] Ummels, B.C.; Gibescu, M.; Pelgrum, E.; Kling, W.L.; Brand, A.J.; "Impacts of Wind Power on Thermal Generation Unit Commitment and Dispatch," *IEEE Trans. On Energy Conversion*, vol. 22, Issue 1, March 2007, pp. 44 – 51.

[19] Chun-Lung, C.; "Optimal Wind–Thermal Generating Unit Commitment," *IEEE Trans. On Energy Conversion*, vol. 23, Issue 1, March 2008, pp. 273 – 280.

[20] Hetzer, J.; Yu, D.C.; Bhattarai, K.; "An Economic Dispatch Model Incorporating Wind Power," *IEEE Trans. On Energy Conversion*, vol. 23, Issue 2, June 2008, pp. 603 – 611.

[21] Hernandez-Aramburo, C.A.; Green, T.C.; Mugniot, N.; "Fuel consumption minimization of a microgrid," *IEEE Trans. on Industry Applications*, vol. 41, Issue 3, May-June 2005, pp. 673 – 681.

[22] Clerc, M., *Particle Swarm Optimization*. Wiley, John & Sons, 2008.

[23] Lee, K.Y.; El-Sharkawi, M.A.; *Modern Heuristic Optimization Techniques: Theory and applications to power systems*, John Wiley & Sons, IEEE press, Piscataway, NJ, 2008.

[24] Guda S.R.; Wang, C.; Nehrir M.H.; "Modeling of Microturbine Power Generation Systems," *Electric Power Components and Systems*, vol. 34, 2006, pp. 1027-1041.

[25] Antoniou, A.; Lu, W.S.; *Practical Optimization: Algorithms and Engineering Applications*. Springer Science & Business Media B.V., 2007, ch. 15.

[26] Available online: http://tonto.eia.doe.gov/oog/info/ngw/ngupdate.asp

[27] Azmy, A.M.; Erlich, I.; "Online Optimal Management of PEM Fuel Cells Using Neural Networks," *IEEE Trans. on Power Delivery*, vol. 29, No. 2, , Apr. 2005, pp. 1051–1058.

[28] Orero, S.O.; Irving, M.R.; "Large scale unit commitment using a hybrid genetic algorithm," *International Journal of Electrical Power & Energy systems*., vol. 19, No. 1, 1997, pp. 45–55.

[29] U.S. Dept. of Energy, Office of Energy Efficiency and Renewable Energy, "Summary of results from testing a 30-kW-microturbine and combined heat and power (CHP) system", DOE/EE-0316, 2007.

[30] Wang, C.; "Modeling and control of hybrid wind/photovoltaic/fuel cell distributed generation systems," Ph.D. Dissertation, Montana State University, Bozeman, MT, 2006.

[31] MATLAB/Simulink SimPowerSystems Documentation, Available on line: http://www.mathworks.com/

[32] Kennedy, J.; Eberhart, R.C.; "Particle swarm optimization", *Proceedings*, IEEE international conference on neural networks, 1995, pp. 39–43.

[33] Del Valle, Y.; Venayagamoorthy, G.K.; Mohagheghi, S.; Hernandez, J.-C.; Harley, R.G.; "Particle Swarm Optimization: Basic Concepts, Variants and Applications in Power Systems", *IEEE Trans. on Evolutionary Computation*, vol. 12, Issue 2, Apr. 2008, pp. 171–195.

[34] Nehrir, M.H.; LaMeres, B.J.; Venkataramanan, G.; Gerez, V.; Alvarado, L.A.; "An approach to evaluate the general performance of stand-alone wind/photovoltaic generation systems", *IEEE Trans. On Energy conversion*, vol. 15, Issue. 4, Dec. 2000, pp. 433–439.

[35] Pop, V.; Bergveld, H.J.; Danilov, D.; Regtien, Paul P.L.; Notten, Peter H.L.; *Battery Management Systems: Accurate State-of-Charge Indication for Battery-Powered Applications*. Springer Science & Business Media B.V., 2008, page: 23.37.

[36] Cahill, J.; Ritland, K.; Kelly, W.; "Description of electric energy use in single family residences in the Pacific Northwest 1986-1992," Office of Energy Resources, Bonneville Power Administration, December 1992, Portland, OR.

[37] Online, Pacific Northwest Cooperative Agricultural Weather Network, AgriMet Historical Dayfile Data Access, Deer Lodge, MT (DRLM), http://www.usbr.gov/pn/agrimet/webaghrread.html.

[38] Masters, G.M.; *Renewable and Efficient Electric Power Systems*, Wiley, 2004.

ACKNOWLEDGMENT

The authors wish to acknowledge the valuable discussions they have had with Dr. Donald Hammerstrom and Dr. Ram Sastry of the Pacific Northwest National Laboratory and Dr. John Sheppard from the Computer Science Department at Montana State University.

BIOGRAPHIES

S. Ali Pourmousavi (S'07) is a Ph.D. student in the Electrical and Computer Engineering (ECE) Department at Montana State University.

M. Hashem Nehrir (M'88–SM'89–F'10) is a professor of ECE at Montana State University.

Christopher M. Colson (S'06) is a Ph.D. student in the ECE Department at Montana State University.

Caisheng Wang (M'02–SM'08) is a faulty member in the ECE Department and Division of Engineering Technology at Wayne State University, Detroit, MI.